NASA TECHNICAL MEMORANDUM

NASA TM X-2477

NASA TM X-2477

COMPARISON OF TEMPERATURE DATA FROM A FOUR-VANE STATIC CASCADE AND A RESEARCH GAS TURBINE ENGINE FOR A CHORDWISE-FINNED, IMPINGEMENT- AND FILM-COOLED VANE

by Herbert J. Gladden, John N. B. Livingood, and Daniel J. Gauntner

Lewis Research Center
Cleveland, Ohio 44135

NATIONAL AERONAUTICS AND SPACE ADMINISTRATION • WASHINGTON, D. C. • FEBRUARY 1972

1. Report No.	2. Government Accession No.	3. Recipient's Catalog No.
NASA TM X-2477		

4. Title and Subtitle	5. Report Date
COMPARISON OF TEMPERATURE DATA FROM A FOUR-VANE STATIC CASCADE AND A RESEARCH GAS TURBINE ENGINE FOR A CHORDWISE-FINNED, IMPINGEMENT- AND FILM-COOLED VANE	February 1972
	6. Performing Organization Code

7. Author(s)	8. Performing Organization Report No.
Herbert J. Gladden, John N. B. Livingood, and Daniel J. Gauntner	E-6597
	10. Work Unit No. 764-74

9. Performing Organization Name and Address	11. Contract or Grant No.
Lewis Research Center National Aeronautics and Space Administration Cleveland, Ohio 44135	
	13. Type of Report and Period Covered
12. Sponsoring Agency Name and Address	Technical Memorandum
National Aeronautics and Space Administration Washington, D.C. 20546	14. Sponsoring Agency Code

15. Supplementary Notes

16. Abstract

Experimental heat-transfer data obtained for a chordwise-finned, impingement- and film-cooled turbine vane tested in a four-vane static cascade to a gas temperature and a gas pressure of 1505 K (2250° F) and 55.2 N/cm^2 (80 psia), respectively, are presented. Average and local vane temperatures are correlated and compared with correlations of temperature data obtained from tests of the same vane in a modified J-75 turbojet engine. The measured vane temperatures obtained from these tests in the two test stands are also compared with analytically determined temperatures.

17. Key Words (Suggested by Author(s))	18. Distribution Statement
Turbine cooling Impingement cooling Film cooling Chordwise fins Engine and cascade comparison	Unclassified - unlimited

19. Security Classif. (of this report)	20. Security Classif. (of this page)	21. No. of Pages	22. Price*
Unclassified	Unclassified	33	$3.00

* For sale by the National Technical Information Service, Springfield, Virginia 22151

COMPARISON OF TEMPERATURE DATA FROM A FOUR-VANE STATIC CASCADE AND A RESEARCH GAS TURBINE ENGINE FOR A CHORDWISE-FINNED, IMPINGEMENT- AND FILM-COOLED VANE

by Herbert J. Gladden, John N. B. Livingood, and Daniel J. Gauntner

Lewis Research Center

SUMMARY

An experimental investigation of the heat-transfer characteristics of a chordwise-finned, impingement- and film-cooled turbine vane operated in a four-vane static cascade to a gas temperature and a gas pressure of 1505 K (2250° F) and 55.2 N/cm^2 (80 psia), respectively, is discussed. Both average and local vane midspan temperatures are correlated for a wide range of operating conditions. These correlations are compared with correlations obtained from tests of the same vane in a modified J-75 turbojet engine for similar operating conditions. Analytically determined vane temperatures are also compared with measured vane temperatures obtained in both the cascade and the engine.

For the range of coolant- to gas-flow ratios of interest, it was found that the average vane temperature difference ratio (gas minus average vane temperature divided by gas minus coolant temperature) for the engine was approximately 0.9 times that for the cascade. By using a similar ratio to correlate local temperature data, it was found that the engine vane leading-edge temperatures exceeded those of the cascade vane by about 200 K (360° F) at the design coolant- to gas-flow ratio of 0.05. For the remaining regions of the vane, the cascade vane temperatures exceeded those of the engine vane by a maximum of 60 K (108° F). Differences in gas stream turbulence and radiation and gas stream temperature profiles between the engine and the cascade were attributed as the reasons for the high leading-edge engine vane temperatures. It was found from the experimental data that, in order to account for these effects, the leading-edge gas-to-vane heat-transfer coefficients for the cascade should be increased by a factor of about 1.35 to obtain a similar coefficient for the engine.

Analytical and experimental average midspan vane temperatures were compared for selected conditions, and agreement was within 4.5 percent for both engine and cascade vanes. Analytical and experimental local midspan vane temperatures for these selected conditions showed agreements between 0 and 22 percent.

The results of the comparisons presented herein indicate that vane temperature data obtained in this cascade were representative of vane temperature data obtained with the J-75 engine, with the exception of the leading-edge region.

INTRODUCTION

A chordwise-finned, impingement- and film-cooled turbine vane was operated in both a four-vane static cascade and a modified J-75 turbojet engine at the NASA Lewis Research Center. The temperature data obtained from these tests are compared. Calculated and measured vane temperatures are also compared for similar operating conditions of the cascade and the engine.

Methods for correlating heat-transfer data for cooled turbine vanes and blades are discussed in references 1 and 2. Several correlation methods are derived in reference 1 and applied to data obtained for an impingement-, convection-, and film-cooled vane tested in the cascade. Reference 2 applies the correlations to a chordwise-finned, impingement- and film-cooled vane operated in the engine. In each case it was found that the simplest correlation, a plot of the ratio of gas temperature minus metal temperature to gas temperature minus coolant temperature against the coolant- to gas-flow ratio, was as good as, or better than, the more complicated correlations derived in reference 1. A method for calculating vane temperatures is also discussed and applied in references 1 and 2.

The present report presents and compares the correlations of vane temperatures obtained in a static cascade and in an engine, using the identical configuration in each case. In addition, methods of correcting correlations obtained in the cascade which will permit a more accurate prediction of the vane performance in an engine are discussed.

Cascade tests were run over the following ranges of variables: gas temperatures from 811 to 1505 K (1000° to 2250° F), gas pressures from 13.8 to 55.2 N/cm^2 (20 to 80 psia), coolant temperatures from 300 to 922 K (80° to 1200° F), and ratios of coolant to gas flow from 0.03 to 0.14. Engine tests were run over the following ranges of variables: gas temperatures from 1033 to 1644 K (1400° to 2500° F), gas pressures near 31 N/cm^2 (45 psia), coolant temperatures from 300 to 700 K (80° to 800° F), and ratios of coolant to gas flow up to 0.15. Only cascade and engine data for comparable sets of operating conditions are compared in this report.

APPARATUS

Cascade Description

The cascade was designed for continuous operation at gas conditions of 1644 K (2500° F) and 103.4 N/cm^2 (150 psia). A detailed description of the cascade is presented in reference 3. The test section was an annular section of a vane row and contained four vanes and five flow channels. A plan view of the cascade test section is shown in figure 1(a). In figure 1(b), the installed vane pack is shown. The two central

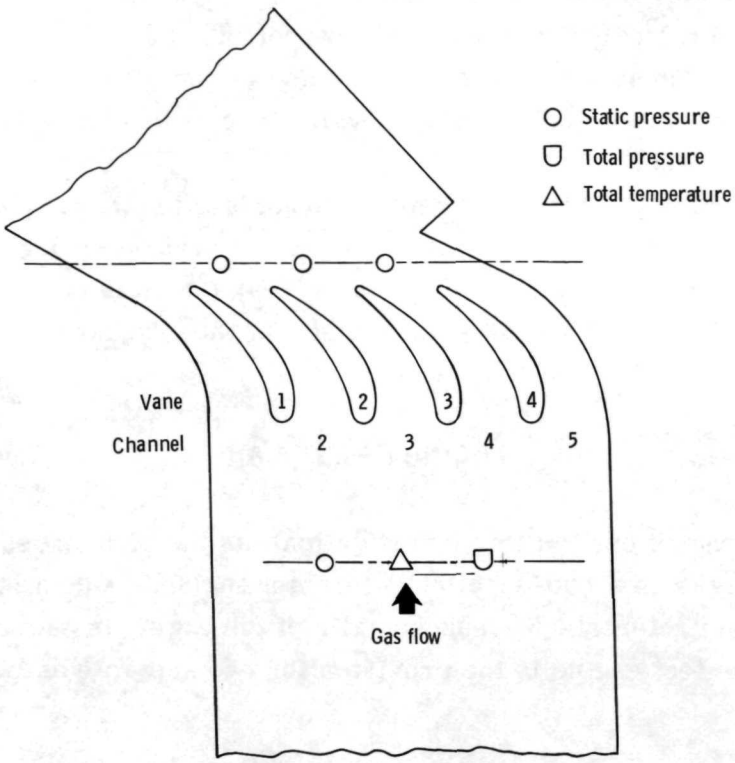

(a) Plan view

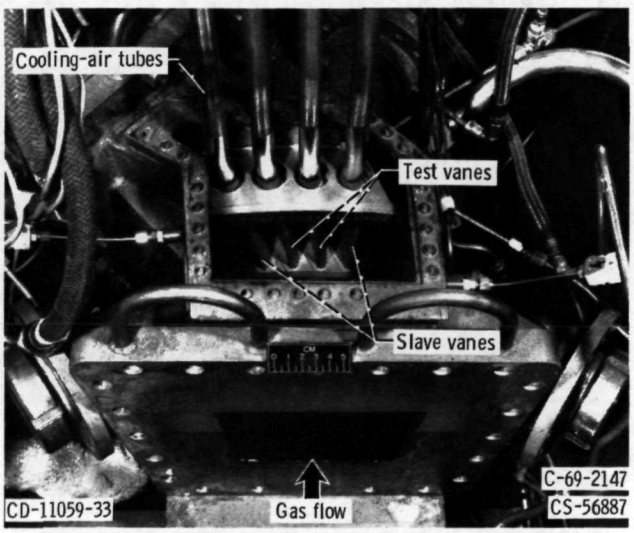

(b) Cascade test section with cover removed.

Figure 1. - Static cascade.

vanes shown in figure 1(b) were test vanes. The two test vanes were supplied by a common cooling-air system, and the cooling air from this system could be preheated to approximately 922 K (1200° F) to simulate compressor bleed air. The two outer vanes, used to provide flow channels for the test vanes and to serve as radiation shields between the test vanes and the water-cooled cascade walls, are each supplied by a separate cooling-air supply system.

For low gas temperature tests, the main burner section was replaced by a spool piece and combustion gas was then supplied to the test section through an auxiliary burner system at temperatures up to 922 K (1200° F); the main burner could operate to 1644 K (2500° F). Reference 1 shows a schematic of the auxiliary burner system.

Engine Description

The research engine used in this investigation was the high-pressure spool and combustor assembly from a two-spool J-75 turbojet engine. A detailed description of the engine is given in reference 3. A schematic of the engine is shown in figure 2. The major feature of the test engine is the provision for two separate and distinct cooling-

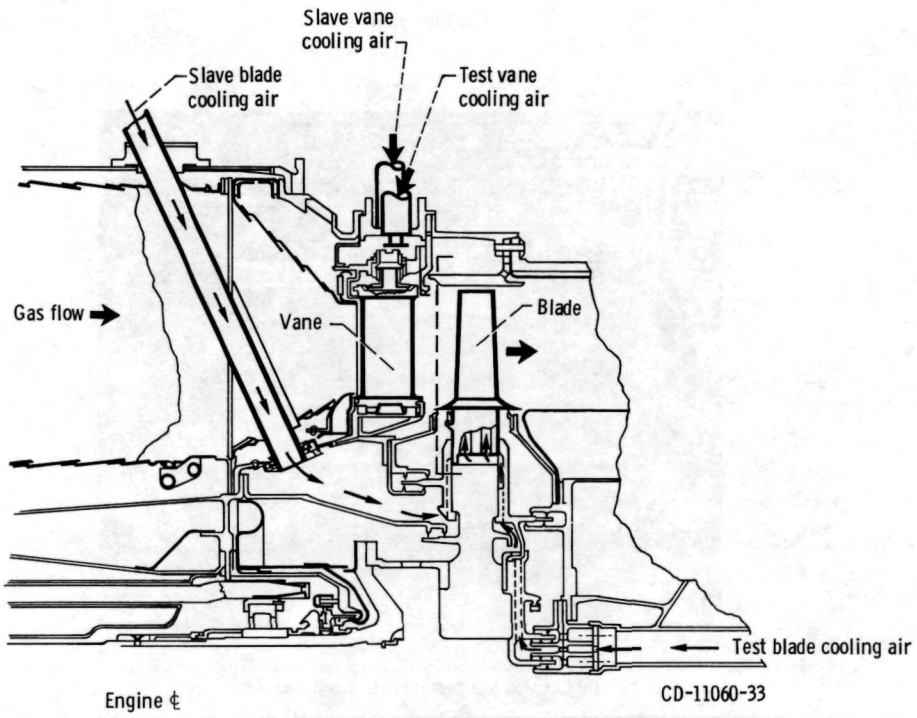

Figure 2. - Turbine cooling research engine.

air systems in the twisted-vane stator assembly and a similar dual cooling-air supply system for the twisted-blade turbine rotor assembly.

The complete turbine stator assembly consisted of 72 vanes. In the research engine, a group of five vanes served as the test vanes. Cooling air was supplied to these vanes from a laboratory air system independent of the system which supplied cooling air to the remaining 67 slave vanes. A similar dual cooling system was used for the rotor and the rotor blades.

Vane Description

A schematic diagram of the NASA-designed vane tested is shown in figure 3. The vane span was 10.2 centimeters (4 in.), and the midspan chord length was 6.4 centimeters (2.5 in.). Cooling air entered the vane from the supply tube located at the tip. The cooling air was ducted into a central cavity as shown in figure 3. From this central

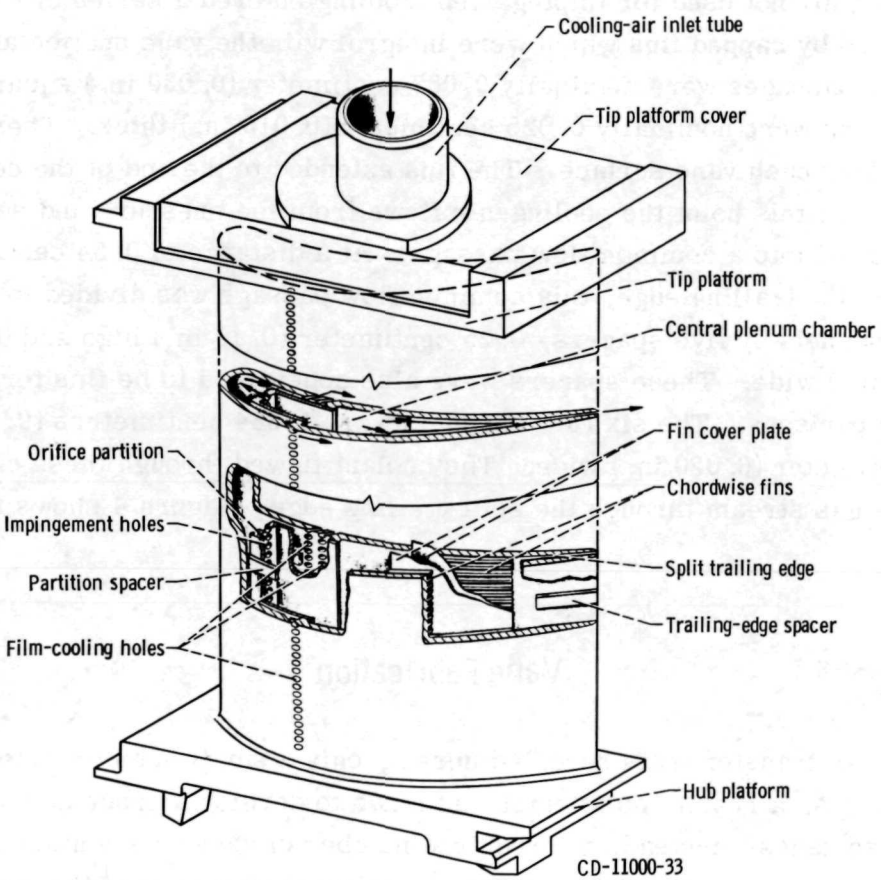

Figure 3. - Cutaway drawing of test vane.

cavity some of the cooling air passed through a row of 46 impingement holes in the orifice partition (fig. 3) to impingement cool the vane leading edge. These holes were 0.127 centimeter (0.050 in.) in diameter and were spaced 0.203 centimeter (0.080 in.) apart; the orifice partition was 0.668 centimeter (0.263 in.) from the inside surface. The cooling air, after impinging on the internal leading-edge surface, flowed chordwise adjacent to the vane suction and pressure surfaces and exited through film-cooling holes located about 1.78 centimeters (0.7 in.) downstream from the stagnation point. There were five spacers 0.25 centimeter (0.1 in.) wide by 0.076 centimeter (0.03 in.) high in each flow path, which formed six flow channels. These spacers were considered fins for subsequent analytical comparisons. The film-cooling holes on the suction surface were a single row of 59 holes, 0.064 centimeter (0.025 in.) in diameter and spaced 0.158 centimeter (0.062 in.) apart, exiting at a 28° angle to the vane surface. Two rows of holes exited on the pressure surface. There were 58 and 59 holes in the two rows and were 0.071 centimeter (0.028 in.) in diameter and spaced 0.158 centimeter (0.062 in.) apart; the holes in the two rows were staggered. Both rows exited at 40° angles to the vane surface.

The cooling air not used for impingement cooling entered a series of chordwise passages formed by capped fins which were integral with the vane suction and pressure surfaces. The passages were nominally 0.067 centimeter (0.030 in.) square in cross section. The fins were nominally 0.025 centimeter (0.010 in.) thick. There were 92 passages along each vane surface. The fins extended to the end of the central plenum chamber. At this point the cooling-air flows from the pressure and suction surfaces reconverged into a common flow passage. At a distance of 0.64 centimeter (0.25 in.) from the trailing edge, this common flow passage was divided into six equally spaced flow channels by five spacers, 0.25 centimeter (0.10 in.) high and 0.051 centimeter (0.020 in.) wide. These spacers were also considered to be fins for subsequent analytical comparisons. The six flow channels were 1.384 centimeters (0.545 in.) high and 0.051 centimeter (0.020 in.) wide. The coolant flowed through these channels and exited into the gas stream through the split trailing edge. Figure 4 shows the finished test vane.

Vane Fabrication

For the heat-transfer tests reported herein, only a small number of test vanes were required. As a result, no attempt was made to develop a procedure for mass producing these vanes. Instead, the required number of vanes were made as follows: Solid, one-piece vanes having the approximate external geometry of the test vane airfoil and hub and tip platforms were vacuum cast of Udimet 700. Two solid castings were re-

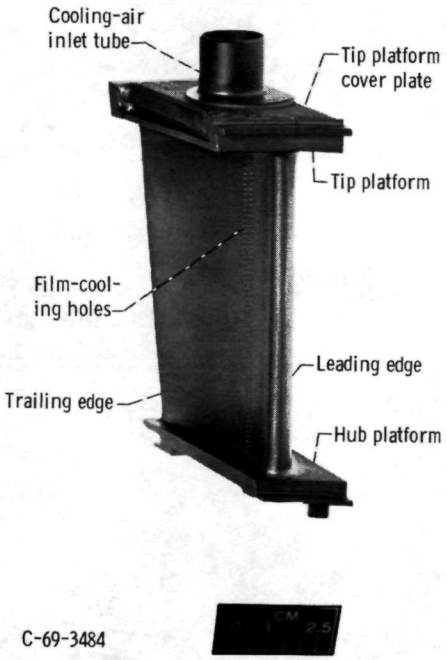

Figure 4. - Test vane assembly showing the pressure surface.

quired to produce one final test vane assembly. The castings were electrical discharge machined to obtain the final internal and external contours. One casting was machined to provide the suction-side geometry, and a second casting was machined to provide the pressure-side geometry. Contoured sheets of 0.013-centimeter (0.005-in.) thick L 605 material were furnace brazed to the edges of the chordwise fins to form the square-cross-section cooling passages. The suction and pressure surface subassemblies were then electron beam welded at the mating faces of the airfoil and the hub and tip platforms.

INSTRUMENTATION

For the cascade tests, each of the two test vanes was instrumented with 25 Chromel-Alumel thermocouples embedded in the walls of the airfoils. Thirteen of these were located at the vane midspan and six each at the hub and tip sections located 1.63 centimeters (0.64 in.) from the respective platforms. For the engine tests, there were three instrumented vanes in the five-test-vane group. A total of 25 thermocouples were also used; 14 were located at the vane midspan section, four at the hub, and seven at the tip. Because of space limitations in bringing thermocouple leads through the vane assembly

and because of structural considerations, the maximum number of thermocouples installed on any one vane in the engine was seven. The fourteen midspan thermocouples were installed on three center test vanes (a leading-edge thermocouple was installed on each of two vanes). For convenience, and for comparison purposes with results from the cascade tests, a composite layout of the midspan engine vane thermocouple locations is shown in figure 5. Each of the cascade vanes and the engine composite vane had the same number of thermocouples installed in similar positions. The construction of the thermocouples is discussed in reference 4.

Inlet cooling-air temperature and pressure and inlet combustion-gas temperature and pressure were measured on both the cascade and the engine. Other required operational instrumentation is discussed in reference 3.

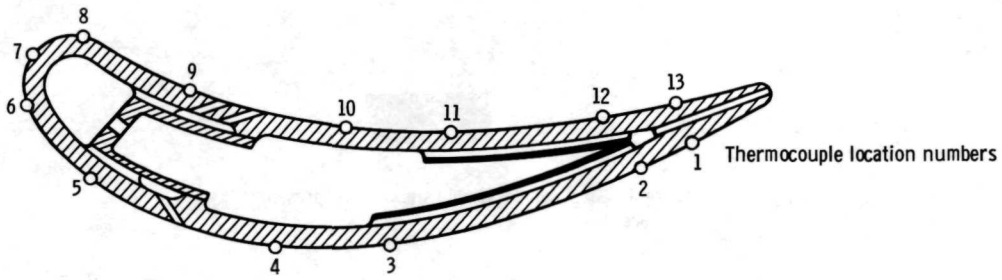

Figure 5. - Midspan thermocouple locations on test vane.

TEST PROCEDURE

Cascade Tests

Cascade tests were made over the range of operating conditions given in table I. The desired combustion gas flow rate, pressure level, and exit static- to total-pressure ratio were established by adjusting inlet and exhaust throttle valves while maintaining the desired total inlet temperature by an automatic temperature controller. For control purposes, the hub and tip exit static pressures were averaged and the average was ratioed to the inlet total pressure (assumed equal to the exit total pressure). When the desired combustion gas conditions were established, the cooling flow rate was varied in a stepwise manner from test point to test point at a given coolant inlet temperature. The coolant- to gas-flow ratios ranged from about 0.03 to 0.14.

Several of the cascade data test points were established based on the similarity consideration detailed in reference 5. These data points were taken at 811 K (1000° F) gas temperature and 300 K (80° F) coolant temperature and scaled up to 1505 K (2250° F) gas

temperature and 550 K (530° F) coolant temperature. Data were also taken for similarity comparisons at the same gas temperatures but at coolant temperatures of 400 and 700 K (260° and 800° F), respectively.

Engine Tests

Engine tests were run over the range of operating conditions given in table II. A test series consisted of a group of test points made at a given nominal average turbine inlet temperature and a given nominal coolant-air supply temperature but at different coolant flow rates. Engine speed was allowed to vary so that the nominal average turbine inlet temperature could be maintained over a wide range of coolant flow rates. Where simultaneous testing of vanes and blades was conducted, combined changes in vane and blade coolant flow rates resulted in engine speed changes of 200 to 500 rpm for some test series. The normal operating procedure was to start a series of test points with the highest coolant flow rate to the test vanes (and test blades, if installed). During most of the testing, the slave vanes and blades were purposely overcooled to preserve life. Between test points, the test vane coolant flow rate was reduced by an incremental step until a maximum local vane temperature of about 1255 K (1800° F) was reached. This temperature was considered to be the maximum safe operating temperature for the vane material. Test vane coolant- to gas-flow ratios up to 0. 15 were covered during the engine testing. Reading of gas and coolant conditions of temperature, pressure, and weight flow and of vane metal temperatures were made at each test point after equilibrium conditions had been reached.

ANALYSIS METHODS

Evaluation of Gas-Side Parameters

In order to predict metal temperatures for the chordwise-finned, impingement- and film-cooled vane considered herein, it is necessary to know certain external vane parameters. These are discussed in detail in reference 1 and briefly summarized in the following paragraphs.

Pressure distribution. - The pressure distribution around the vane profile may be obtained from experimental measurements or by a calculation method. Experimentally measured pressure distributions around a solid vane of the same airfoil shape as the chordwise-finned vane were obtained when the vane was installed in the cascade and in the engine; these distributions are presented in the section RESULTS AND DISCUSSION. Several methods of calculating the pressure distribution around an airfoil are also avail-

able (refs. 6 and 7). In reference 8 excellent agreement between calculated and measured pressure distributions for this vane profile in the cascade are shown.

Convection gas-to-vane heat-transfer coefficients. - For the vane leading edge, the equation for flow over a cylinder was used; this equation is (ref. 9, p. 373).

$$Nu_g = 1.14\ Re^{0.5} Pr^{0.4}\left(1 - \left|\frac{\theta}{90}\right|^3\right) \tag{1}$$

where θ is the angle measured from the stagnation point and $-80^\circ < \theta < 80^\circ$, and where $Nu_g = h_g d_g / k_g$.

For the other convection-heated parts of the vane, the equation for turbulent flow over a flat plate was used; it is (ref. 10, p. 198)

$$Nu_g = 0.0296\ Re^{0.8} Pr^{1/3} \tag{2}$$

where $Nu_g = h_g x / k_g$. Equations (1) and (2) were based on the following reference temperature (ref. 11, p. 270):

$$T_{ref} = 0.28\ T_{st} + 0.5\ T_w + 0.22\ T_{ge} \tag{3}$$

Effective gas temperatures. - The local effective gas temperature was obtained from

$$T_{ge} = T'' - \frac{(1 - \Lambda) W_y^2}{2 g C_p J} \tag{4}$$

where T'' is the relative total temperature, W_y is the relative local velocity, and Λ is the recovery factor. For turbulent flow, $\Lambda = Pr^{1/3}$; and for laminar flow, $\Lambda = Pr^{1/2}$. For a vane, the relative values are identical to the absolute values so that in equation (4) T'' becomes T' and W_y becomes v.

Film-cooling effectiveness. - The film-cooling effectiveness is usually expressed in the form

$$\eta = C\,(Re)_{c,s}^{l_1}\left(\frac{x}{Ms}\right)^{-l_2} \tag{5}$$

The equivalent slot width s was obtained by equating the total area of the film-cooling holes on a given surface to that of a slot whose length was the vane span. For the vane considered herein, the following equations from reference 12 were used:

$$\eta = -0.00001\left(\frac{x}{Ms}\right)^{1.952} + 0.5 \qquad \text{for the suction surface} \tag{6}$$

and

$$\eta = -0.026\left(\frac{x}{Ms}\right)^{0.498} + 0.5 \qquad \text{for the pressure surface} \tag{7}$$

These values of η were then used in

$$\eta = \frac{T_{ge} - T_{aw}}{T_{ge} - T_{c,s}} \tag{8}$$

to obtain the adiabatic wall temperature T_{aw} (ref. 13, p. 250). This temperature was used instead of T_{ge} for determining the heat flux to a film-cooled surface.

Vane-to-Coolant Heat-Transfer Coefficients

For convectively cooled regions of the vane that do not contain chordwise fins, the vane-to-coolant heat-transfer coefficients were obtained from the correlation (ref. 9, p. 347)

$$Nu = 0.021\ Re^{0.8} Pr^{0.333} \tag{9}$$

When the heat-transfer surface was increased by the addition of fins, the fin effectiveness was included. Including the fin effectiveness altered the coefficient in equation (9); the resulting equation was

$$Nu = 0.021\ \eta_b Re^{0.8} Pr^{0.333} \tag{10}$$

where η_b is the fin effectiveness. The specific values are given in the next section.

For the impingement-cooled leading-edge region, a local heat-transfer correlation is obtained by combining correlations from references 14 and 15. The ratio of local to average heat-transfer coefficients is obtained from reference 14. To obtain this ratio, an expression for the local Stanton number is divided by an expression for the average Stanton number, both expressions being evaluated at an optimum spacing between the jet

hole and the heat-transfer surface. The resulting relation expressed in terms of Nusselt numbers is

$$\frac{Nu(x)}{\overline{Nu}} = 0.475\left(\frac{4x}{\pi d_c}\right)^{-0.475}$$

where x is measured from the stagnation point. The average Nusselt number is obtained from reference 15 and appears in a different form as follows:

$$\overline{Nu} = 0.36\ Re^{0.62}\left(\frac{2d_n}{\pi d_c}\right)^{0.38}$$

The product of these two expressions will yield an expression for the local heat-transfer coefficient around the inner surface of the leading edge. The correlation is

$$Nu = 0.0364\ Re^{0.62}{}_x{}^{-0.475} \tag{11}$$

The Reynolds number in equation (11) was based on the nozzle or hole diameter.

Predicted Vane Temperature

The flow distribution of the coolant as it passes through the vane internal cooling passages must be known to predict local vane temperatures. To determine these flow distributions, a one-dimensional compressible flow network is used to simulate the internal cooling configuration. Experimentally measured pressures and flow distributions made in separate cold flow tests for the chordwise vane and presented in reference 2 were used. By use of these data, flow characteristics such as inlet and exit losses and friction pressure drops were determined. These flow characteristics were then used to establish the required flow coefficients in the one-dimensional network which would result in local flows which matched the local flows for the cases that were experimentally measured.

With the flow coefficients now known, the flow distribution through the vane in either the cascade or the engine can be determined. By use of available measured external pressures, the measured total coolant flow, and the measured inlet coolant temperature, the flow distribution through the vane can be determined by iterating on the inlet pressure until the calculated total flow converges to the measured total flow.

To predict vane temperatures, other quantities must be known. From the discussions already presented, the effective gas temperature distribution, the gas-to-vane

heat-transfer coefficients, and the vane-to-coolant heat-transfer coefficients can be estimated. For the heat-transfer calculations, a nodal network for the vane (including fins) was established. Then, the combined flow and heat-transfer programs were used to determine the vane temperatures. Iteration between flow and heat transfer was required until the calculated vane temperatures converge and the total calculated flow matched the total measured flow to a predetermined convergence criterion.

Five regions of the vane contained fins or simulated fins to augment the convection cooling of that particular segment and are discussed in the section Vane Description. The fin effectiveness for the leading-edge spacers was 1.6; for the midchord fins, 3.02; and for the trailing-edge spacers, 1.58. The convection equation was also modified for entrance effects for the five regions. The form of the entrance effect term was taken from reference 16:

$$\text{Entrance effects} \equiv 1 + \frac{1.4}{y/d_h} \tag{12}$$

Experimental Vane Temperature Correlation

Several methods for correlating experimental vane heat-transfer data were developed in reference 1 and were used to analyze cascade vane data in reference 1 and engine vane data in reference 2. In each case, it was found that the simple correlation, a plot of the temperature difference ratio φ against the coolant- to gas-flow ratio $\dot{w}_c/\dot{w}_g$ was about as accurate as the more complicated correlations presented in reference 1. As a result, only the simplified correlation φ against $\dot{w}_c/\dot{w}_g$ is considered herein.

The simplified correlation was applied to both average and local midspan vane temperatures. The inlet coolant temperature was used for T_c and the midspan turbine inlet temperature was used for T_{ge} in the determination of φ. Total gas flow per vane channel and total coolant flow rates per vane were used for the coolant- to gas-flow ratios $\dot{w}_c/\dot{w}_g$. These are the same procedures used in references 1 and 2.

RESULTS AND DISCUSSION

Comparison of Measured Pressure Distributions

Experimental pressure distributions around the solid vane profile were obtained in the cascade and the research engine. The results of these two investigations are taken from references 2 and 8 and are presented in figures 6(a) and (b) as plots of the ratio of

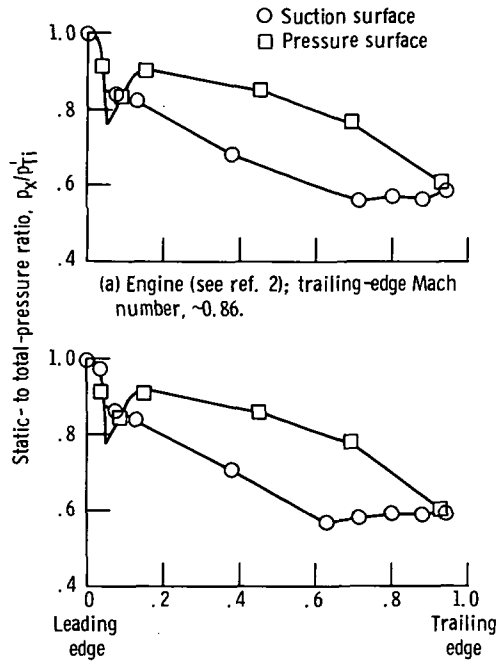

Figure 6. - Experimental pressure distribution around solid vane with test vane profile when installed in the engine and in the cascade.

static- to total-pressure against the dimensionless surface distance from the vane stagnation point. (The results shown are for the midspan position only.) The trailing-edge midspan Mach number for the engine tests was 0.86 and for the cascade tests was 0.85. Except for this slight variation in trailing-edge Mach number, the distributions are very similar. The measured pressure distribution obtained for the vane in the cascade is predicted very well in reference 8 by use of the analytical method discussed in reference 7. Reference 8 also presents the spanwise midchannel trailing-edge static-pressure distribution in the cascade and concludes from the data that the gas flow was not fully three dimensional. In effect, the static-pressure gradient (from hub to tip) was considerably less in the cascade than the analytical gradient obtained for the engine. Qualitatively, this phenomenon caused the coolant flow distribution through the cascade vane to be somewhat different than the flow distribution through the engine vane.

Comparison of Gas Temperature Profiles

Plots of the measured turbine inlet temperature for the cascade and the engine are presented in figure 7. For the cascade tests, the gas temperature was measured in

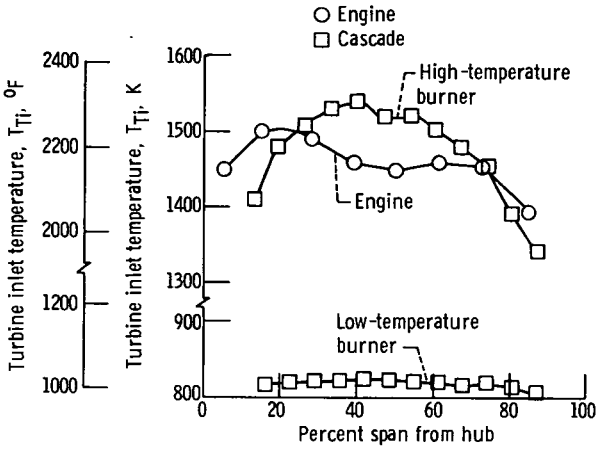

Figure 7. - Typical spanwise turbine inlet temperature distribution for the engine and each of the cascade burners.

front of channel 3 (see fig. 1(a)). Spanwise distributions for the high-temperature burner and the low-temperature burner are designated by the square symbols.

For the engine, the turbine inlet temperature was measured by circumferentially spaced turbine inlet probes which traversed in a radial direction. Corresponding radial positions on each of the probes were averaged to obtain the turbine inlet temperature profile shown in figure 7.

The test vanes were not located directly behind the temperature measuring probes. Therefore, the vanes may have been subjected to a different gas temperature profile than that shown in figure 7.

Comparison of Measured Chordwise Temperature Distributions

Operation of the cascade and the engine under identical gas and coolant conditions was impractical. Hence, in order to compare measured chordwise vane temperatures, it was necessary to select a cascade run and an engine run whose operating conditions were nominally the same. For this purpose, measured chordwise vane temperatures for the following operating conditions were selected:

	Turbine inlet temperature, T_{Ti}		Coolant inlet temperature, $T_{c,i}$		Coolant-to gas-flow ratio, $\dot{w}_c/\dot{w}_g$	Average wall temperature, $\overline{T}_w$		Temperature difference ratio, $\overline{\varphi}$
	K	°F	K	°F		K	°F	
Cascade	1503	2245	295	72	0.050	960	1268	0.45
Engine	1458	2164	298	76	.053	911	1181	.47

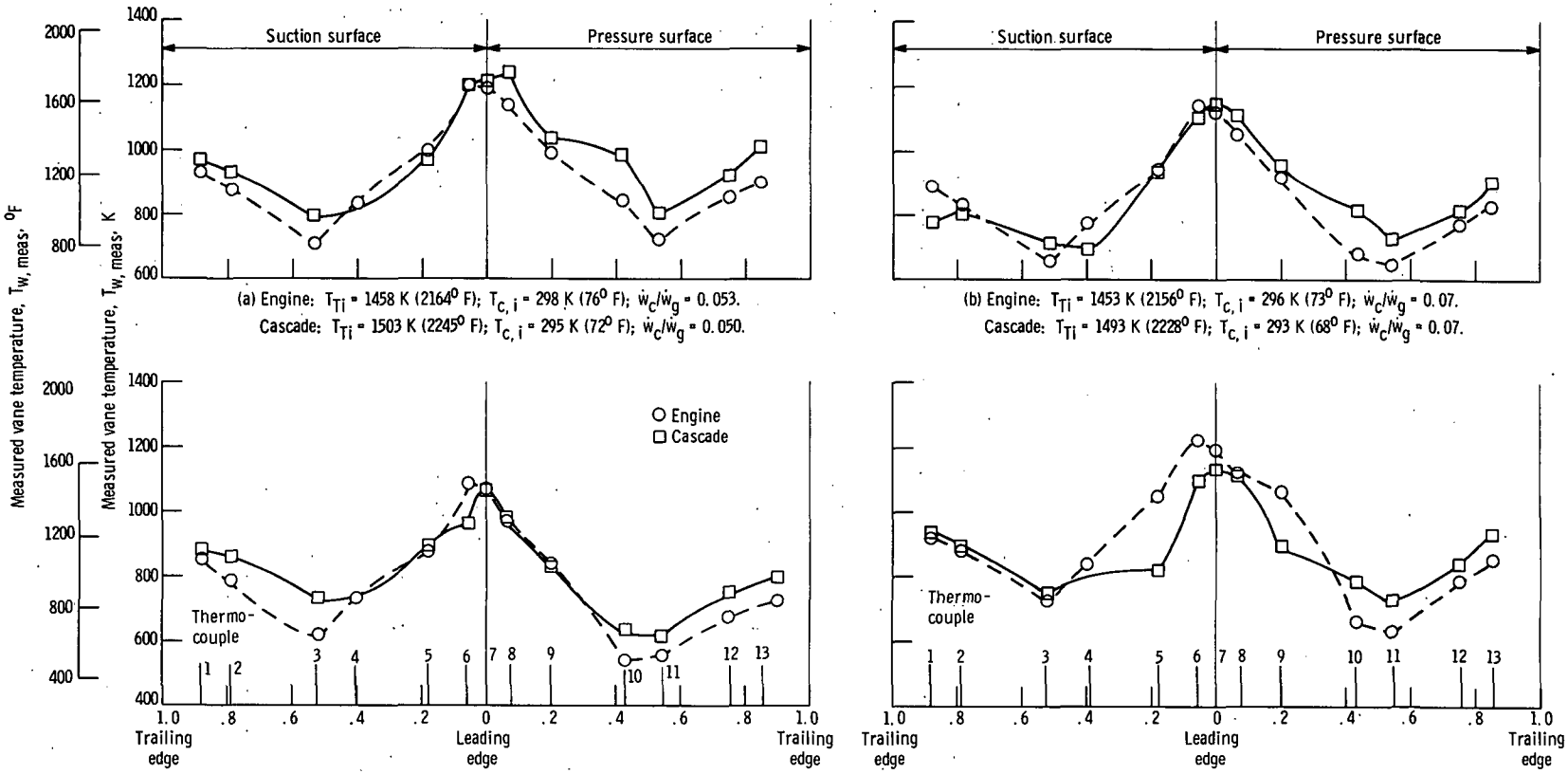

(a) Engine: T_{Ti} = 1458 K (2164° F); $T_{c,i}$ = 298 K (76° F); $\dot{w}_c/\dot{w}_g$ = 0.053.
Cascade: T_{Ti} = 1503 K (2245° F); $T_{c,i}$ = 295 K (72° F); $\dot{w}_c/\dot{w}_g$ = 0.050.

(b) Engine: T_{Ti} = 1453 K (2156° F); $T_{c,i}$ = 296 K (73° F); $\dot{w}_c/\dot{w}_g$ = 0.07.
Cascade: T_{Ti} = 1493 K (2228° F); $T_{c,i}$ = 293 K (68° F); $\dot{w}_c/\dot{w}_g$ = 0.07.

(c) Engine: T_{Ti} = 1469 K (2184° F); $T_{c,i}$ = 295 K (72° F); $\dot{w}_c/\dot{w}_g$ = 0.109.
Cascade: T_{Ti} = 1504 K (2247° F); $T_{c,i}$ = 311 K (100° F); $\dot{w}_c/\dot{w}_g$ = 0.101.

(d) Engine: T_{Ti} = 1581 K (2386° F); $T_{c,i}$ = 295 K (71° F); $\dot{w}_c/\dot{w}_g$ = 0.083.
Cascade: T_{Ti} = 1555 K (2340° F); $T_{c,i}$ = 301 K (82° F); $\dot{w}_c/\dot{w}_g$ = 0.076.

Figure 8. - Comparison of measured vane temperatures in cascade and engine, where T_{Ti} is turbine inlet temperature, $T_{c,i}$ is coolant inlet temperature, and $\dot{w}_c/\dot{w}_g$ is the ratio of coolant flow to gas flow.

The measured vane temperatures are shown in figure 8(a); cascade data are denoted by the square symbols and engine data by the circular symbols. The majority of the cascade vane temperatures were higher than those of the engine vane, as was expected, since the cascade turbine inlet temperature was higher than the engine turbine inlet temperature at the midspan position (fig. 7). Figure 8(a) shows that, in the vane leading-edge region, the differences in the vane temperatures decreased. This may be attributed to the effect of stream turbulence and radiation in the vane leading-edge region of engine. Turbulence and flame radiation increase the gas-to-vane heat-transfer coefficient and, hence, the engine vane temperatures in the vane leading-edge region. These effects of turbulence and radiation are discussed in the section Comparison of Gas-to-Vane Heat-Transfer Coefficients in connection with predicted vane temperatures.

Figures 8(b) to (d) show three other comparisons of measured vane temperatures obtained from operating the two facilities under other nominally similar conditions. The results for these comparisons are similar to those obtained from figure 8(a). Dimensionless temperature data correlations and chordwise profiles based on these correlations are presented in the following sections.

As mentioned in the discussion of pressure distributions around the vanes, the difference in the spanwise static-pressure gradients may have an effect on the coolant flow distribution in each vane. This effect may contribute to the change in the relation of engine and cascade temperatures between the leading-edge region and the vane afterbody. The magnitude of this effect is unknown and this conjecture is offered for qualitative discussion purposes only.

Comparison of Vane Midspan Average Temperature Difference Ratio

The average vane midspan temperature data were correlated by plotting the average temperature difference ratio $\overline{\varphi}$ against the ratio of coolant to gas flow $\dot{w}_c/\dot{w}_g$. These plots are presented in figure 9; only data for the cascade vane are shown on the figure. Data for the engine vane are presented in reference 2. Average correlating equations for each vane (in the cascade and in the engine) are shown in figure 9. By observing the data points in figure 9, it can be seen that there is a trend in the spread of the data with cooling-air temperature. The higher coolant temperatures result in higher values of $\overline{\varphi}$. It therefore appears that the correlation parameter $\overline{\varphi}$ against coolant- to gas-flow ratio $\dot{w}_c/\dot{w}_g$ does not completely account for the coolant temperature.

By ratioing the engine correlation to the cascade correlation, it follows that

$$\overline{\varphi}_{eng} = \overline{\varphi}_{cas}\left[1 - \frac{0.024}{(\dot{w}_c/\dot{w}_g)^{0.8} + 0.114}\right] \tag{13}$$

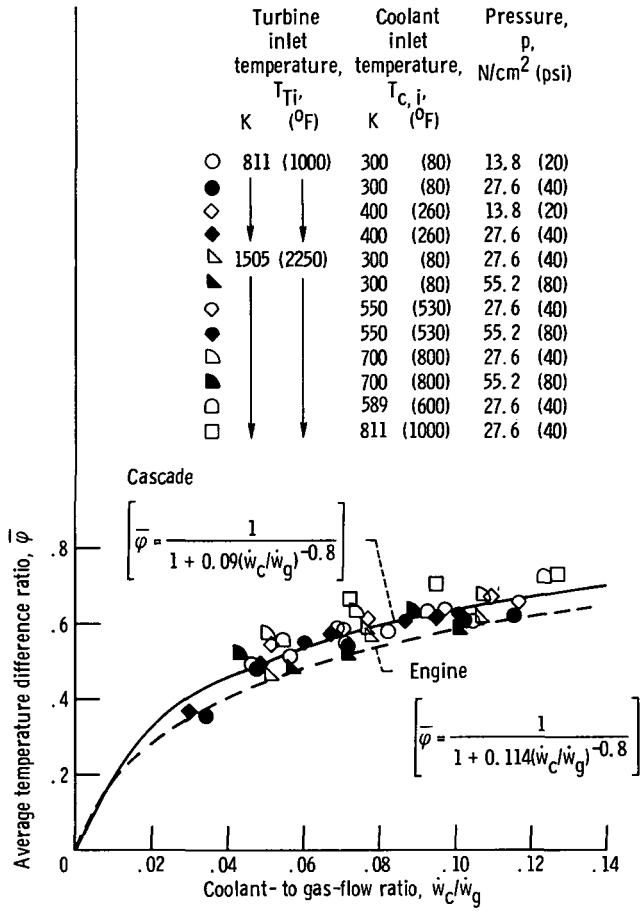

Figure 9. - Comparison at average vane midspan temperature correlations for the cascade and the engine, for various cascade operating conditions.

The ratio of $\varphi_{eng}/\varphi_{cas}$ was evaluated and found to be approximately 0.9 for the coolant- to gas-flow ratio range of interest.

Comparison of Vane Midspan Local Temperature Difference Ratio

Plots of φ_x against $\dot{w}_c/\dot{w}_g$ were made for all thermocouple locations shown in figure 5 for both the cascade and the engine. Four thermocouple locations were selected for representative comparisons of local values of φ_x. The cascade data and the best-fit correlation curves through the data are shown in figures 10(a) to (d). Also shown in the figures are the engine correlation best-fit curves taken from reference 2. The particular thermocouple location under consideration is shown in the small vane sketch for each of the four positions considered. Also, the equation of the cascade best-fit curve is shown in each sublegend. For the thermocouples located in the leading-edge

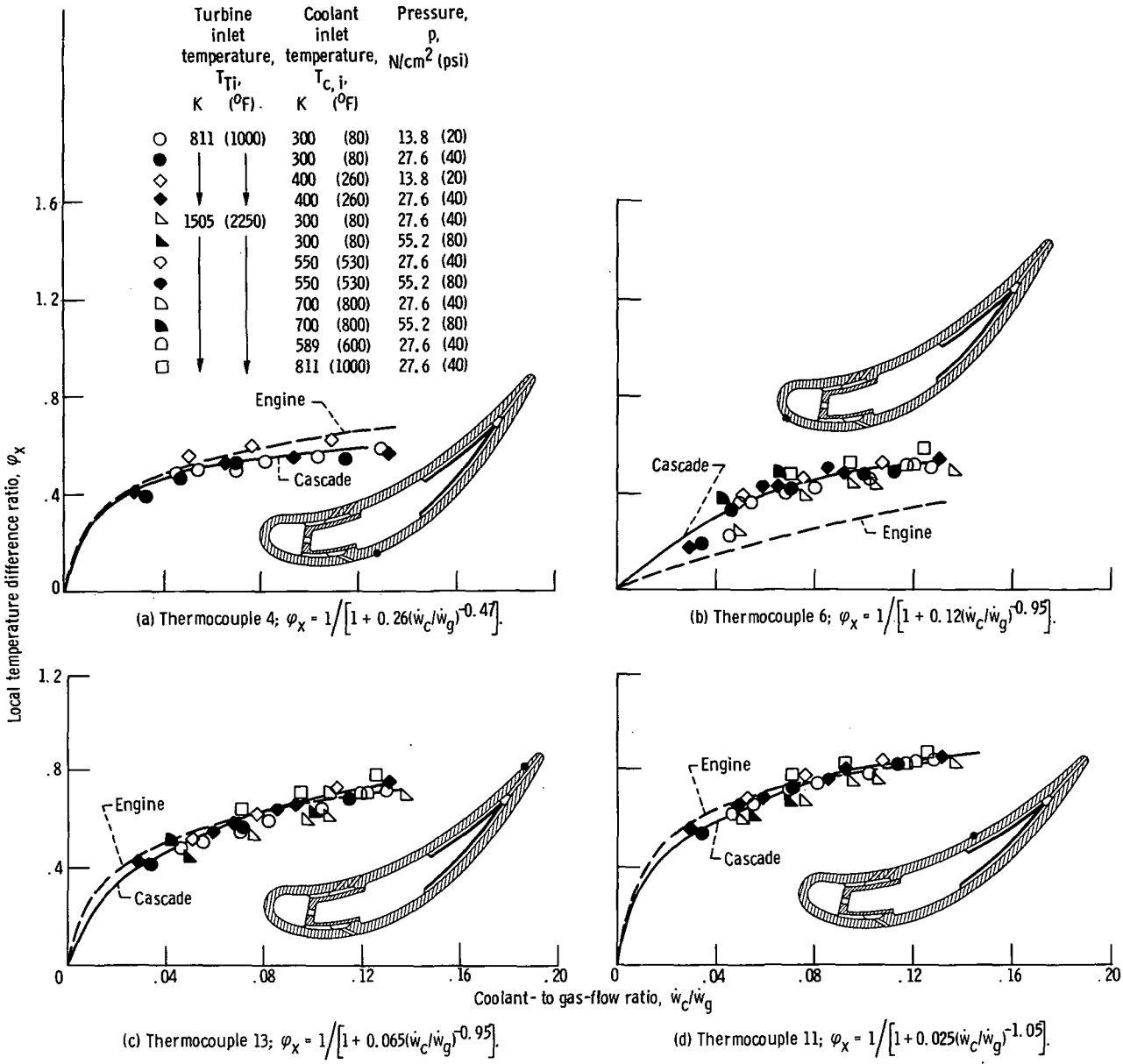

Figure 10. - Comparison of local vane midspan temperature correlation for the cascade and the engine, for various cascade operating conditions.

region of the vane, the local values of φ_x for the cascade vane are higher than those for the engine vane for similar operating conditions (fig. 10(b)), indicating that the leading-edge vane temperatures in the engine are higher than those temperatures in the cascade. This is attributed to the effect of turbulence of the main gas stream and radiation from the combustion process; turbulence and radiation increase the engine vane gas-to-vane heat-transfer coefficients and, in turn, the engine vane temperatures in the leading-edge region.

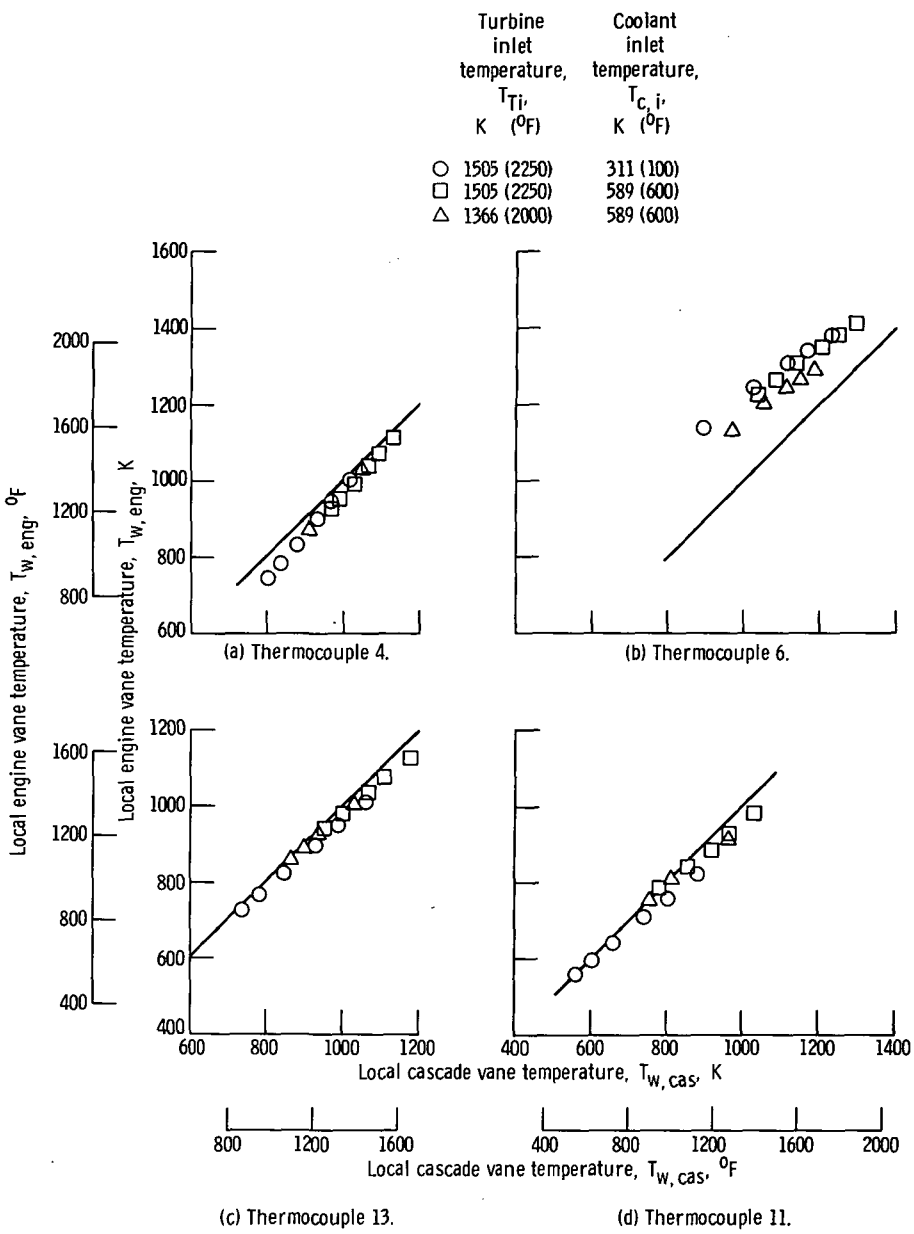

Figure 11. - Comparison of local vane temperatures in engine and cascade as determined by the correlation equations. Coolant- to gas-flow ratio, 0.03 to 0.11.

For the other thermocouple locations on the cascade and engine vanes, the local values of φ_x are similar but with the engine values being somewhat higher in the majority of cases. This indicates the engine vane temperatures were generally lower than the cascade vane temperatures for similar conditions with the exception of the leading edge. These trends were previously noted in the plots of measured chordwise vane temperatures for the cascade and engine vanes (fig. 8).

Comparison of Vane Midspan Temperatures Determined by the Local Temperature Difference Ratio Correlations

Four thermocouple locations (the same locations shown on fig. 10) were selected to compare local vane temperatures as determined by the best-fit correlations of the engine and the cascade. Figures 11(a) to (d) show engine vane temperatures as a function of cascade vane temperatures for three assumed combinations of gas and coolant temperatures and a range of coolant- to gas-flow ratios. These assumed conditions are shown in figure 11. The maximum deviation between the temperature data from the two vanes was 60 K (108° F) for thermocouple locations 4, 11, and 13. For thermocouple location 6, near the leading edge, the maximum difference was about 240 K (432° F) at 0.03 coolant flow ratio, 311 K (100° F) coolant temperature, and 1505 K (2250° F) gas temperature. At the design coolant- to gas-flow ratio of 0.05 and the preceding temperature conditions, the maximum deviation was 200 K (360° F).

Comparison of Vane Midspan Temperature Distributions Determined by the Local Temperature Difference Ratio Correlations

Chordwise vane temperature distributions were calculated by use of the local correlation equations for both the cascade and the engine vanes for a turbine inlet temperature of 1533 K (2300° F), a coolant inlet temperature of 589 K (600° F), and two ratios of coolant to gas flow. The results are shown in figure 12(a) for a ratio of coolant to gas flow of 0.05 and in figure 12(b) for a ratio of coolant to gas flow of 0.08. These curves show the same trends between the engine and cascade as previously discussed. All thermocouple locations compare within 72 K (130° F) except for locations 5 and 6 (x/L of 0.18 and 0.055, respectively, on the suction surface). Because of the magnitude of the temperature differences between these values, one might suspect that some of the experimental vane temperature measurements may be inaccurate. No evidence was found to indicate whether the engine temperatures or the cascade temperatures were in error.

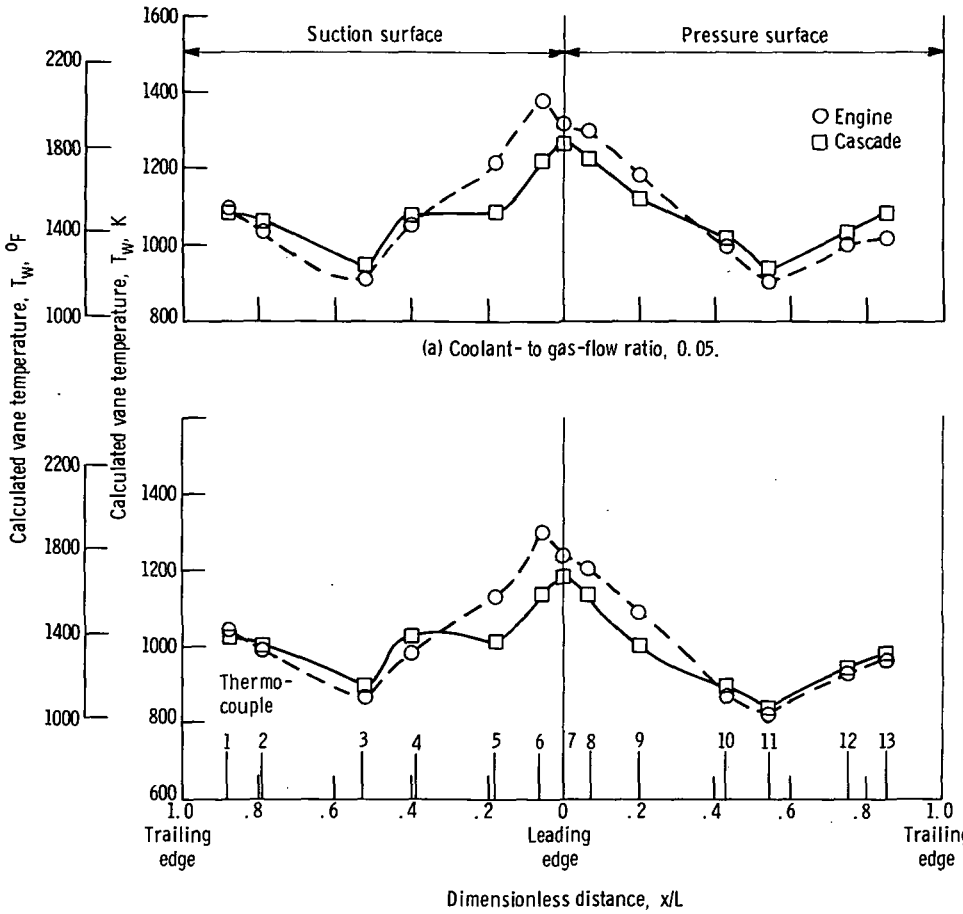

(a) Coolant- to gas-flow ratio, 0.05.

(b) Coolant- to gas-flow ratio, 0.08.

Figure 12. - Comparison of calculated chordwise temperature distributions determined by the local temperature difference ratio correlations for the cascade and the engine. Turbine inlet temperature, 1533 K (2300° F); coolant temperature, 589 K (600° F).

Comparison of Gas-to-Vane Heat-Transfer Coefficients

If it is assumed that the inlet total gas temperature and pressure are the same for the cascade and the engine, use of equations (1) and (2) permits a rapid comparison of the gas-to-vane heat-transfer coefficients based on the pressure distributions for the cascade and the engine. For the same gas temperature, the property values of the gas will be fixed; and since the vane geometry is fixed, it follows that the heat-transfer coefficients depend only on a power of ρv (the Reynolds number with the surface distance, and gas viscosity deleted since both are fixed). For example, from equation (2) it follows that

$$\frac{h_{g,\,cas}}{h_{g,\,eng}} = \frac{(\rho v)^{0.8}_{cas}}{(\rho v)^{0.8}_{eng}} = \left\{ \frac{\left(\frac{p_x}{p'_{Ti}}\right)^{(\gamma-1)/\gamma}_{eng} \left[\sqrt{1 - \left(\frac{p_x}{p'_{Ti}}\right)^{(\gamma-1)/\gamma}_{cas}} \right]}{\left(\frac{p_x}{p'_{Ti}}\right)^{(\gamma-1)/\gamma}_{cas} \left[\sqrt{1 - \left(\frac{p_x}{p'_{Ti}}\right)^{(\gamma-1)/\gamma}_{eng}} \right]} \right\}^{0.8} \tag{14}$$

By use of the experimental pressure distributions of figures 6(a) and (b), the ratio of $h_{g,\,cas}/h_{g,\,eng}$ can now be found for constant inlet total gas temperature and pressure. For example, at about $x/L = 0.07$ on the suction surface, $h_{g,\,cas}/h_{g,\,eng}$ was found to be about 0.92; at about $x/L = 0.63$ on the suction surface, $h_{g,\,cas}/h_{g,\,eng}$ equals 0.96. On the pressure surface, figures 6(a) and (b) show essentially the same pressure distributions for the cascade and the engine, and hence the gas-to-vane heat-transfer coefficients on the pressure surface for the cascade and the engine will be essentially the same.

The preceding discussion does not account for the effects of stream turbulence or of radiation. It is known that turbulence does affect gas-to-vane heat-transfer coefficients. The relation between the gas-to-vane heat-transfer coefficients for the cascade and the engine when turbulence and radiation effects are included can be estimated by use of experimental data. The temperature difference ratio φ is expressible as

$$\varphi = \frac{1}{1 + A_r \frac{h_g}{h_c}} \tag{15}$$

where A_r is the ratio of heat-transfer areas between the outside and inside surfaces. Solving for h_c for the cascade and for the engine and equating the two results yields

$$\frac{h_{g,\,eng}}{h_{g,\,cas}} = \left(\frac{\varphi}{1 - \varphi}\right)_{cas} \left(\frac{1 - \varphi}{\varphi}\right)_{eng} \tag{16}$$

For experimental leading-edge temperature data at comparable nominal operating conditions it was found that the ratio of engine to cascade gas-side heat-transfer coefficients $h_{g,\,eng}/h_{g,\,cas}$ was 1.35. Since the values of $h_{g,\,cas}$ are known, values for $h_{g,\,eng}$ may be obtained by multiplying the $h_{g,\,cas}$ leading-edge values by this value of 1.35 in order to account for the effects of turbulence, radiation, and any uncertainty in the gas temperature profile.

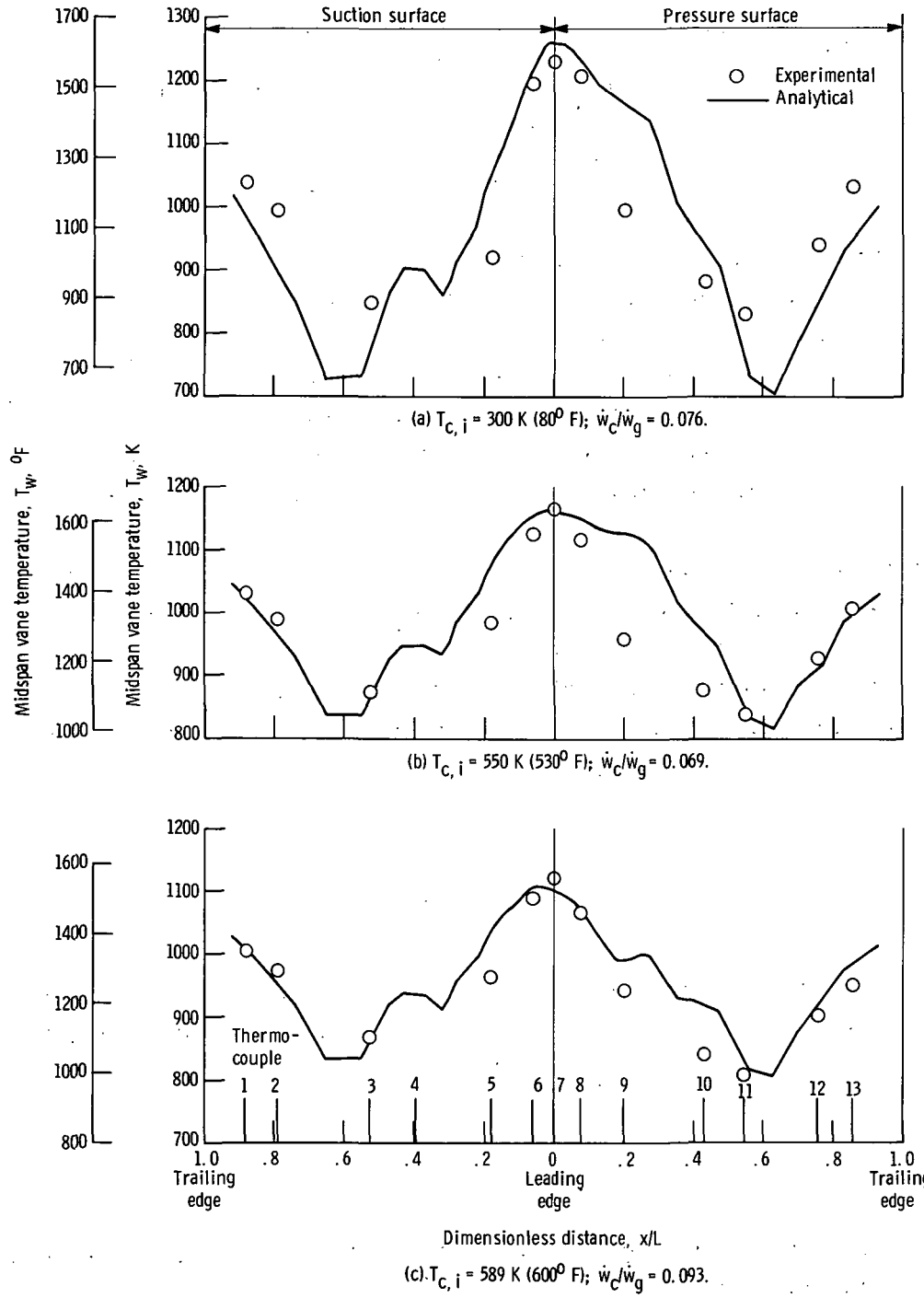

Figure 13. - Comparison of analytical and experimental midspan vane temperatures - cascade. Turbine inlet temperature, 1505 K (2250^o F); $T_{c,i}$ is coolant inlet temperature and $\dot{w}_c/\dot{w}_g$ is coolant-to gas-flow ratio.

Comparison of Experimental and Analytical Midspan Vane Temperature Distributions

Experimental and analytical chordwise temperature profiles for the cascade vane are shown in figures 13(a) to (c) for a range of test conditions. The nominal turbine inlet temperature for the three comparisons is 1505 K (2250° F). The coolant temperatures are 300, 550, and 589 K (80°, 530°, and 600° F); and the coolant- to gas-flow ratios are 0.076, 0.069, and 0.093, respectively.

The experimental vane temperatures agree moderately well with the analytical temperatures for the three cases presented. Leading-edge temperatures (thermocouples 6 to 8, see fig. 5) agreed within ±5 percent or less of the analytical temperatures. The midchord vane temperatures (thermocouples 3, 10, and 11; thermocouple 4 was inoperative during these particular readings) agreed within ±11 percent or less of the analytical values. For the trailing-edge vane temperatures (thermocouples 1, 2, 12, and 13), agreement was within ±3 percent of the analytical temperatures, except in figure 13(a). Here, the deviation was ±11 percent. It is suspected that the analytical flow determination for the reading of figure 13(a) has allowed too much coolant flow through the split trailing edge. This would have the effect of over-cooling the trailing edge, thus accounting for the higher trailing-edge temperature deviation for this one reading.

The last two temperature comparisons (thermocouples 5 and 9) were not as good for the three cases. The maximum deviation for the three readings of figure 13 ranged from +6 to +22 percent. The reason for this deviation is not clear at the present and may be experimental error in the measured temperature.

The average midspan vane temperatures were calculated by averaging the areas under the temperature distribution curves. The distribution curves were established by straight-line fairing between the temperature readings. The average experimental midspan vane temperatures for figures 13(a) to (c) were 860, 958, and 935 K (1088°, 1264°, and 1223° F), respectively. The average analytical temperatures were found to be 864, 998, and 964 K (1096°, 1337°, and 1275° F), respectively. The deviation of the average analytical temperatures from the average experimental temperatures were 4 K (12° F) or 0.5 percent, 40 K (73° F) or 4.5 percent, and 29 K (52° F) or 3.3 percent, for figures 13(a), (b), and (c), respectively.

Analytical temperatures were also found for the engine vane. A plot similar to those of figure 13 is presented in figure 14 for engine temperature data at similar operating conditions with the inlet cooling air at room temperature. The experimental average vane temperature was 842 K (1056° F), while the analytical average was 834 K (1041° F). Thus, the analytical temperature was within 8 K (15° F), or 1 percent of the experimental average temperature.

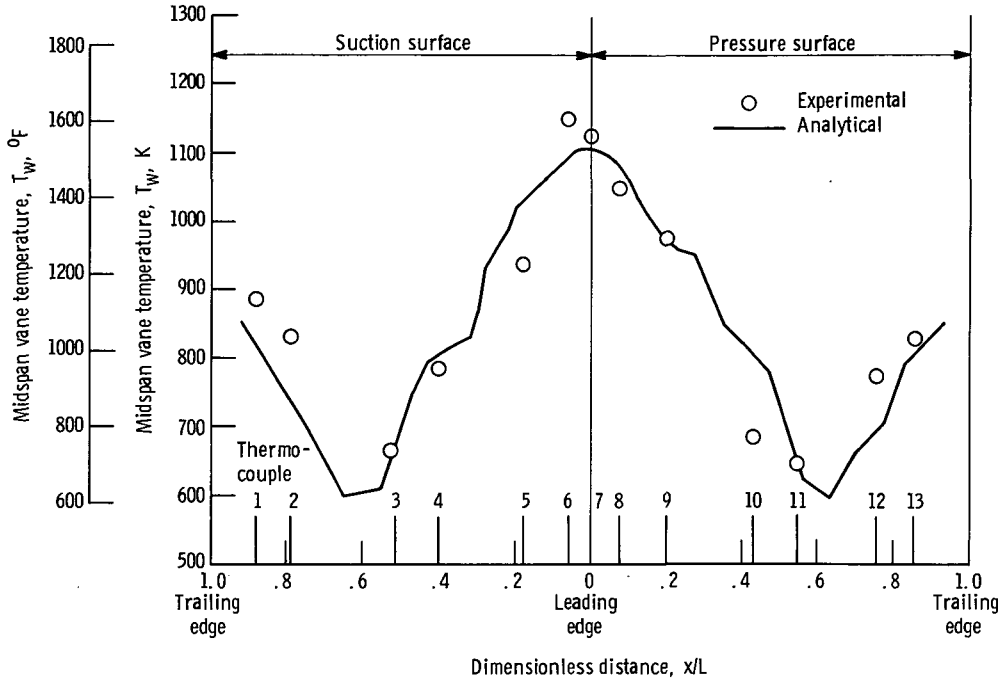

Figure 14. - Comparison of analytical and experimental midspan vane temperatures - engine. Turbine inlet temperature, 1453 K (2156^0 F); turbine inlet temperature, 296 K (73^0 F); coolant-to gas-flow ratio, 0.070.

The deviations of local and average analytical vane temperatures from experimental vane temperatures are explained, in part, by a discussion of the flow and heat-transfer models used in the temperature prediction program. In the program, the flow model determined the cooling-air flow through most of the vane to be in the transitional region. If, at local regions in the vane, the model incorrectly determined transitional flow instead of turbulent flow, the heat-transfer model would determine analytical vane temperatures which are higher than the experimental temperature. Local deviations in the flow model could thus explain the poor comparison of experimental and analytical temperatures at the cascade vane thermocouple locations 5 and 9. This assignment of transitional flow instead of turbulent flow could result if the effective area in the flow model were larger than the actual effective flow area. Thus, good matching of the flow model with the measured flow distribution is necessary to accurately determine local and average vane temperatures.

Another cause for the higher analytical temperatures might be in the gas-side heat-transfer-coefficient distribution. In figures 13 and 14, turbulent values for h_g were used around the vane gas-side, except for one region on the suction side of the cascade vane (fig. 13) which was treated as laminar. This region extended from just past the cylindrical leading edge to the start of the film-cooling holes. It may be that laminar or transitional values of h_g should also be used on other regions of the vane in the cascade.

SUMMARY OF RESULTS

A comparison of results obtained from tests of a chordwise-finned, impingement- and film-cooled test vane in a four-vane static cascade and in a research turbojet engine are summarized as follows:

1. Experimental pressure distributions around a solid vane of the same profile as the test vane were similar in the cascade and engine.

2. For the range of coolant- to gas-flow ratios of interest, the value of the average temperature difference ratio (average gas temperature minus average vane temperature divide by average gas temperature minus coolant temperature) for the engine was found to be approximately 0.9 times the value of the ratio for the cascade.

3. Differences in the effects of gas stream turbulence, flame radiation, and gas stream temperature profiles on the vane leading-edge temperatures between the cascade and the engine could be accounted for by increasing the gas-to-vane heat-transfer coefficients for the cascade vane leading-edge region by a factor of about 1.35 to determine like engine coefficients.

4. Comparisons of vane temperatures as determined by use of the local temperature difference ratios for similar cascade and engine operating conditions indicated (a) maximum deviation of about 60 K (108 ^{o}F) for thermocouple locations other than the leading edge for the full range of coolant- to gas-flow ratios; (b) a nominal temperature deviation at the leading edge of about 200 K (360 ^{o}F) at the design coolant- to gas-flow ratio.

5. Analytical and experimental average vane temperatures for both the cascade and engine vanes agreed within 4.5 percent. Analytical and experimental local vane temperature comparisons ranged from 0 to 22 percent.

6. Results of the comparisons presented herein indicate that vane temperature data obtained in the cascade were representative of the engine vane temperature data with the exception of the leading-edge region.

Lewis Research Center,
National Aeronautics and Space Administration,
Cleveland, Ohio, November 1, 1971,
764-74.

APPENDIX - SYMBOLS

A_r	ratio of areas
C	constant
C_p	specific heat at constant pressure
d	vane leading-edge diameter
d_h	hydraulic diameter
d_n	nozzle diameter
g	gravitational constant
h	heat-transfer coefficient
J	mechanical equivalent of heat
k	thermal conductivity
L	length of vane surface
l_1, l_2	exponents
M	$(\rho v)_c/(\rho v)_g$
Nu	Nusselt number
Pr	Prandtl number
p	pressure
Re	Reynolds number
s	equivalent slot width
T	temperature
W_y	relative velocity
v	velocity
$\dot{w}$	flow rate
x	distance from film-cooling slot; distance from stagnation point along vane internal or external surface
y	distance from entrance of coolant passage
Λ	recovery factor
γ	ratio of specific heats
η	film-cooling effectiveness

η_b fin effectiveness

θ angle measured from stagnation point

φ temperature difference ratio, $(T_{ge} - T_w)/(T_{ge} - T_c)$

ρ density

Subscripts:

aw adiabatic wall

c coolant

cas cascade

eng engine

g gas

ge effective gas

i inlet

meas measured

ref reference

s slot

st static

Ti turbine inlet

w wall

x local

Superscripts:

$\bar{}$ average

' total

'' relative total

REFERENCES

1. Gladden, Herbert J.; Gauntner, Daniel J.; and Livingood, John N. B.: Analysis of Heat-Transfer Tests of an Impingement, Convection, Film Cooled Vane in a Cascade. NASA TM X-2376, 1971.

2. Gauntner, James W.; Lane, Jan M.; Dengler, Robert P.; and Hickel, Robert O.: Experimental Heat-Transfer Results of a Chordwise Finned Turbine Vane with Impingement, Film, and Convection Cooling. NASA TM X-2472, 1972.

3. Calvert, Howard F.; Cochran, Reeves P.; Dengler, Robert P.; Hickel, Robert O.; and Norris, James W.: Turbine Cooling Research Facility. NASA TM X-1927, 1970.

4. Crowl, Robert; and Gladden, Herbert J.: Methods and Procedures for Evaluating, Forming, and Installing Small-Diameter Sheathed Thermocouple Wire and Sheathed Thermocouples. NASA TM X-2377, 1971.

5. Gladden, Herbert J.; and Livingood, John N. B.: Procedure for Scaling of Experimental Turbine Vane Airfoil Temperatures from Low to High Gas Temperature. NASA TN D-6510, 1971.

6. Katsanis, Theodore: Fortran Program for Calculating Transonic Velocities on a Blade-to-Blade Stream Surface on a Turbomachine. NASA TN D-5427, 1969.

7. Katsanis, Theodore; and Dellner, Lois T.: A Quasi-Three-Dimensional Method for Calculating Blade Surface Velocities for an Axial Flow Turbine Blade. NASA TM X-1394, 1967.

8. Gladden, Herbert J.; Dengler, Robert P.; Evans, David G.; and Hippensteele, Steven A.: Aerodynamic Investigation of Four-Vane Cascade Designed for Turbine Cooling Studies. NASA TM X-1954, 1970.

9. Kreith, Frank: Principles of Heat Transfer. International Textbook Co., 1958.

10. Rohsenow, Warren M.; and Choi, Harry Y.: Heat, Mass, and Momentum Transfer. Prentice-Hall, Inc., 1961.

11. Eckert, E. R. G.; and Drake, Robert M., Jr.: Heat and Mass Transfer. Second ed., McGraw-Hill Book Co., Inc., 1959.

12. Burggraf, F.; Murtaugh, J. P.; and Wilton, M. E.: Design and Analysis of Cooled Turbine Blades. Part I - Leading and Trailing Edge Configurations. Rep. R68AEG101, General Electric Co. (NASA CR-54513), Jan. 1, 1968.

13. Kays, William M.: Convective Heat and Mass Transfer. McGraw-Hill Book Co., Inc., 1966.

14. Jenkins, D. E.; and Metzger, C. W.: Local Heat Transfer Characteristics of Concave Cylindrical Surfaces Cooled by Impinging Slot Jets and Lines of Circular Jets with Spacing Ratios 1.25 to 6.67. Rep. TR-694, Arizona State Univ., May 1969.

15. Burggraf, F.: Average Heat Transfer Coefficients with a Row of Air Jets Discharging into a Half Cylinder. M. S. Thesis, Univ. Cincinnati, 1967.

16. McAdams, William H.: Heat Transmission. Third ed., McGraw-Hill Book Co., Inc., 1954.

TABLE I. - SUMMARY OF CASCADE OPERATING CONDITIONS

Combustion gas conditions				Inlet coolant conditions			
Nominal inlet total temperature		Inlet total pressure		Nominal temperature		Coolant-to-gas temperature ratio	Coolant- to gas-flow ratio, $\dot{w}_c/\dot{w}_g$
K	°F	N/cm^2	psia	K	°F		
811	1000	13.8	20	300	80	0.370	0.056 to 0.130
↓	↓	27.6	40	300	80	.370	0.034 to 0.115
		13.8	20	400	260	.493	0.051 to 0.109
		27.6	40	400	260	.493	0.030 to 0.133
1505	2250	27.6	40	300	80	0.199	0.050 to 0.138
↓	↓	55.2	80	300	80	.199	0.055 to 0.101
		27.6	40	550	530	.365	0.050 to 0.116
		55.2	80	550	530	.365	0.060 to 0.101
		27.6	40	700	800	.465	0.050 to 0.107
		55.2	80	700	800	.465	0.043 to 0.088
		27.6	40	589	600	.391	0.054 to 0.123
		27.6	40	811	1000	.539	0.0718 to 0.126

TABLE II. - SUMMARY OF ENGINE OPERATING CONDITIONS

Series	Nominal turbine inlet temperature		Nominal compressor inlet temperature		Nominal cooling-air temperature at vane inlet		Coolant- to gas-flow ratio, $\dot{w}_c/\dot{w}_g$	Range of engine speed, rpm
	K	°F	K	°F	K	°F		
1	1366	2000	450	350	296	73	0.049 to 0.134	7300 to 7700
2	1478	2200	↓	↓	297	75	0.053 to 0.130	7950
3	1561	2350			294	70	0.083 to 0.144	8700
4	1366	2000			478	400	0.081 to 0.110	6850
5	↓	↓			↓	↓	0.041 to 0.079	7100 to 7300
6							0.021 to 0.109	7200 to 7600
7					700	800	0.024 to 0.099	7200 to 7500
8	1033	1400	297	75	299	78	0 to 0.080	6940
9	1366	2000	294	70	299	78	0.05 to 0.11	7920

NASA-Langley, 1972 — 33 E-6597

"The aeronautical and space activities of the United States shall be conducted so as to contribute . . . to the expansion of human knowledge of phenomena in the atmosphere and space. The Administration shall provide for the widest practicable and appropriate dissemination of information concerning its activities and the results thereof."

—NATIONAL AERONAUTICS AND SPACE ACT OF 1958

NASA SCIENTIFIC AND TECHNICAL PUBLICATIONS

TECHNICAL REPORTS: Scientific and technical information considered important, complete, and a lasting contribution to existing knowledge.

TECHNICAL NOTES: Information less broad in scope but nevertheless of importance as a contribution to existing knowledge.

TECHNICAL MEMORANDUMS: Information receiving limited distribution because of preliminary data, security classification, or other reasons.

CONTRACTOR REPORTS: Scientific and technical information generated under a NASA contract or grant and considered an important contribution to existing knowledge.

TECHNICAL TRANSLATIONS: Information published in a foreign language considered to merit NASA distribution in English.

SPECIAL PUBLICATIONS: Information derived from or of value to NASA activities. Publications include conference proceedings, monographs, data compilations, handbooks, sourcebooks, and special bibliographies.

TECHNOLOGY UTILIZATION PUBLICATIONS: Information on technology used by NASA that may be of particular interest in commercial and other non-aerospace applications. Publications include Tech Briefs, Technology Utilization Reports and Technology Surveys.

Details on the availability of these publications may be obtained from:

SCIENTIFIC AND TECHNICAL INFORMATION OFFICE

NATIONAL AERONAUTICS AND SPACE ADMINISTRATION

Washington, D.C. 20546